Scattering Analysis of Active FSS Structures Using Spectral-Element Time-Domain Method

H. Xu, J. Xi and R. S. Chen
Department of Communication Engineering
Nanjing University of Science and Technology , Nanjing , China, 210094

***Abstract*- Active frequency selective surface (FSS) structure is a kind of electromagnetic spatial filter, which has been widely used in the communication and radar systems. The spectral-element time domain method has been used to analyze the scattering characteristic of finite planar FSS structures. It has the advantages of spectral accuracy and block-diagonal mass matrix. This technique is based on Gauss-Lobatto-Legendre polynomials and Galerkin's method is used for spatial discretization. The absorbed boundary condition is employed to truncate the boundary. Numerical results demonstrate the accuracy of the method.**

***Index Terms*- active frequency selective surface, spectral-element time domain method, scattering.**

I. INTRODUCTION

Frequency selective surface is usually made up of metal patches or periodic arrangement of aperture unit on the metal sheet, which has been widely used in communication and radar system. Usually the operating frequency band can not be changed once they are designed and manufactured. As a result, many people have been doing researches on active FSS structures, which has the ability of adjusting their transmission characteristics by using active devices such as PIN diodes[1]-[2].

Time-domain method has been more and more popular in recent years because of their abilities in the analysis of transient electromagnetic fields and the broadband properties of devices. Among these, one popular technique is the finite-element time-domain (FETD) method [3], which is famous for convenient modeling of complex geometries and materials. However, the inversion of the mass matrix makes it cost a lot in calculating. Finite difference time domain (FDTD), on the other hand, has the advantages of simple theory and good generality, but does not suit for complicated objects and media. The spectral-element time-domain (SETD) method, based on Gauss-Lobatto-Legendre polynomials, has the advantages of spectral accuracy and block-diagonal mass matrix and thus has received much attention recently. Moreover, the SETD can be regarded as a special kind of FETD method with different choices of nodal points and quadrature integration points [4].

In this paper, spectral-element time-domain method is employed to compute the scattering characteristic of finite planar active FSS structures with PIN diodes. RCS results of the FSS are presented respectively when it is in ON state and OFF state.

II. FORMULATION

A. Scattering formulation

For the proposed method, we can use the total-field/scattered-field formulation . In the total-field region

$$\nabla\times\left[\frac{1}{\mu}\nabla\times\mathbf{E}^{\mathbf{t}}(\mathbf{r},t)\right]+\varepsilon\frac{\partial^2}{\partial t^2}\mathbf{E}^{\mathbf{t}}(\mathbf{r},t)=0 \qquad (1)$$

while in the scattered-field region

$$\nabla\times\left[\frac{1}{\mu_0}\nabla\times\mathbf{E}^{\mathbf{sc}}(\mathbf{r},t)\right]+\varepsilon_0\frac{\partial^2}{\partial t^2}\mathbf{E}^{\mathbf{sc}}(\mathbf{r},t)=0 \qquad (2)$$

where $\mathbf{E}^{\mathbf{t}}(\mathbf{r},t)=\mathbf{E}^{\mathbf{sc}}(\mathbf{r},t)+\mathbf{E}^{\mathbf{inc}}(\mathbf{r},t)$

The absorbed boundary condition is employed to truncate the boundary

$$\hat{n}\times\left[\frac{1}{\mu_0}\nabla\times\mathbf{E}^{\mathbf{sc}}(\mathbf{r},t)\right]+\gamma\frac{\partial}{\partial t}\left[\hat{n}\times\hat{n}\times\mathbf{E}^{\mathbf{sc}}(\mathbf{r},t)\right]=0 \qquad (3)$$

to discretize the equation , we introduce the Gauss-Lobatto-Legendre points. The Nth- order GLL basis functions in a one-dimensional standard reference element are defined as

$$\Phi_j^{(N)}(\xi)=\frac{1}{N(N+1)L_N(\xi_j)}\frac{\left(1-\xi^2\right)L_N'(\xi)}{\xi-\xi_j} \qquad (4)$$

for j = 0,…,N, where $L_N(\xi)$ is the Nth-order Legendre polynomial and $L_N'(\xi)$ is its derivative. The grid points ξ_j are chosen as the GLL points, i.e.,the (N+1) roots of equation $\left(1-\xi_j^{\,2}\right)L_N'(\xi_j)=0$

On a 3-D standard cubic reference element, we use vector basis functions

$$\mathbf{\Phi}_{rst}^{\xi} = \hat{\xi}\phi_r^{(N\xi)}(\xi)\phi_s^{(N\eta)}(\eta)\phi_t^{(N\zeta)}(\zeta)$$
$$\mathbf{\Phi}_{rst}^{\eta} = \hat{\eta}\phi_r^{(N\xi)}(\xi)\phi_s^{(N\eta)}(\eta)\phi_t^{(N\zeta)}(\zeta) \qquad (5)$$
$$\mathbf{\Phi}_{rst}^{\zeta} = \hat{\varsigma}\phi_r^{(N\xi)}(\xi)\phi_s^{(N\eta)}(\eta)\phi_t^{(N\zeta)}(\zeta)$$

as shown in Fig.1, where N_ξ, N_η and N_ς are the interpolation orders of the reference domain along ξ, η and ς parametric coordinates, respectively [5].

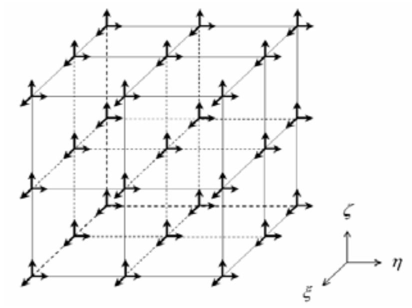

Fig. 1. Vector basis functions in reference element. The second-order basis functions are shown here

When constructing a curl-conforming vector basis functions , we use the appropriate mapping given by

$$\tilde{\mathbf{\Phi}} = \mathbf{J}^{-1}\mathbf{\Phi}$$
$$\nabla\times\tilde{\mathbf{\Phi}} = \frac{1}{|\mathbf{J}|}\mathbf{J}^{T}\nabla\times\mathbf{\Phi} \qquad (6)$$

where $\mathbf{J}$ is the Jacobian matrix defined as

$$\mathbf{J} = \begin{bmatrix} \frac{\partial x}{\partial \xi} & \frac{\partial y}{\partial \xi} & \frac{\partial z}{\partial \xi} \\ \frac{\partial x}{\partial \eta} & \frac{\partial y}{\partial \eta} & \frac{\partial z}{\partial \eta} \\ \frac{\partial x}{\partial \zeta} & \frac{\partial y}{\partial \zeta} & \frac{\partial z}{\partial \zeta} \end{bmatrix} \qquad (7)$$

In the reference element, the electric field can be represented by the tensor product of Lagrange–Legendre interpolation polynomials as

$$\begin{aligned}\mathbf{E}(\xi,\eta,\zeta) &= \sum_{r=0}^{N\xi}\sum_{s=0}^{N\eta}\sum_{t=0}^{N\zeta}\mathbf{\Phi}_{rst}^{\xi}e^{\xi}(\xi_r,\eta_s,\zeta_t) \\ &+ \sum_{r=0}^{N\xi}\sum_{s=0}^{N\eta}\sum_{t=0}^{N\zeta}\mathbf{\Phi}_{rst}^{\eta}e^{\eta}(\xi_r,\eta_s,\zeta_t) \\ &+ \sum_{r=0}^{N\xi}\sum_{s=0}^{N\eta}\sum_{t=0}^{N\zeta}\mathbf{\Phi}_{rst}^{\zeta}e^{\zeta}(\xi_r,\eta_s,\zeta_t) = \sum_{j=1}^{N}\mathbf{\Phi}_j e_j\end{aligned} \qquad (8)$$

after employing the basis function and Galerkin's method,

$$\int\left\{\varepsilon\mathbf{\Phi_i}\cdot\frac{\partial^2}{\partial t^2}\mathbf{E^t}+\frac{1}{\mu}(\nabla\times\mathbf{\Phi_i})\cdot\left(\nabla\times\mathbf{E^t}\right)\right\}dV_t$$
$$+\int\left\{\varepsilon_0\mathbf{\Phi_i}\cdot\frac{\partial^2}{\partial t^2}\mathbf{E^{sc}}+\frac{1}{\mu_0}(\nabla\times\mathbf{\Phi_i})\cdot\left(\nabla\times\mathbf{E^{sc}}\right)\right\}dV_s$$
$$+\sqrt{\frac{\varepsilon_0}{\mu_0}}\int\left(\hat{n}\times\mathbf{\Phi_i}\right)\cdot\left(\hat{n}\times\frac{\partial}{\partial t}\mathbf{E^{sc}}\right)dS-\frac{1}{\mu_0}\int\left(\hat{n}\times\mathbf{\Phi_i}\right)\cdot\left(\nabla\times\mathbf{E^{inc}}\right)dS=0$$
(9)

B. Active frequency selective surface

In this paper, the active frequency selective surface is mainly focused on FSS structure with PIN diodes.

We also start from the wave equation，for simplification, after the Galerkin' s method, we can get

$$[A]E+[B]\frac{dE}{dt}+[C]\frac{d^2E}{dt^2}+[D]E'+[E]E''+[M]\frac{\partial J}{\partial t}=0 \quad (10)$$

$$[M]_{ij} = \iint_S\left(\int_l \bar{N}_i\cdot\hat{n}_y dy\right)dS \qquad (11)$$

Using the central difference,

$$\begin{aligned}&\left(0.5\Delta tT_q+T\right)E_1^{n+1} = \left(2T-\Delta t^2(S+T_p)\right)E_1^{n}+\left(0.5\Delta tT_q-T\right) \\ &E_1^{n-1}-\left(\Delta t^2S_1\right)E_1^{'n}-\left(\Delta t^2S_{th}\right)E_1^{''n}-\Delta t^2M\frac{\partial J_d}{\partial t}\end{aligned} \qquad (12)$$

expanding the M matrix,

$$[TT]E_1^{n+1} = [SS]E_1^{n\cdots\cdots}-\Delta t^2 h\,\mathrm{int}\,w_m\frac{\partial I_d}{\partial t} \qquad (13)$$

In the forward bias condition, the diode presents a resistance in series with the package inductance while in the reverse bias the circuit becomes a parallel combination of and in series with ,for simplification, we can also use a series RLC circuit model

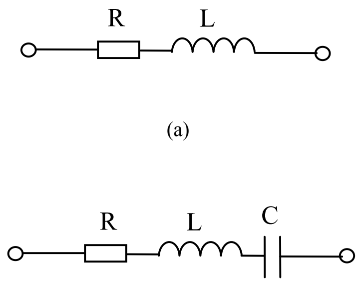

(a)

(b)

Fig. 2. The PIN diode (a) the forward bias equivalent circuit (b) the reverse bias equivalent circuit

In the forward bias condition,

$$V_d = L\frac{\partial I_d}{\partial t} + I_d R \tag{14}$$

Using the forward difference,

$$\frac{V_d^{n+1}+V_d^n}{2} = L\frac{I_d^{n+1}-I_d^n}{\Delta t} + \frac{I_d^{n+1}+I_d^n}{2}R = \left(L+\frac{\Delta t}{2}R\right)\cdot\frac{\partial I_d}{\partial t} + I_d^n R \tag{15}$$

Take (15) into (13), we ultimately obtain the time iteration scheme

$$\begin{aligned}[TT]e_1^{n+1} &= [SS]e_1^{n\ldots\ldots} - \Delta t^2 h\,\text{int}\, w_m \frac{\partial I_d}{\partial t} \\ &= [SS]e_1^{n\ldots\ldots} - \Delta t^2 h\,\text{int}\, w_m\left[\frac{V_d^{n+1}+V_d^n-2I_d^n R}{2L+\Delta t R}\right]\end{aligned} \tag{16}$$

The derivation of reverse bias condition is the same as that of the forward bias.

The above scheme calculates the near field. To obtain far field data, we introduce an artificial boundary S_{far} inside the solution domain, which can be placed at or near the surface of the scatterer. The equivalent electric and magnetic currents can be determined from the fields calculated by SETD[6].

$$\begin{aligned}\mathbf{J}(\mathbf{r},t) &= \hat{n}\times\mathbf{H}(\mathbf{r},t) = -\hat{n}\times\frac{1}{\mu}\int_0^t \nabla\times\mathbf{E}(\mathbf{r},t)dt \\ \mathbf{M}(\mathbf{r},t) &= -\hat{n}\times\mathbf{E}(\mathbf{r},t)\end{aligned} \tag{17}$$

The following surface integrals are computed

$$\begin{aligned}\mathbf{L}(\mathbf{r},t) &= \iint_{S_{far}} \mathbf{M}\left(\mathbf{r}',t+c^{-1}\hat{r}\cdot\mathbf{r}'\right)ds' \\ \mathbf{N}(\mathbf{r},t) &= \iint_{S_{far}} \mathbf{J}\left(\mathbf{r}',t+c^{-1}\hat{r}\cdot\mathbf{r}'\right)ds'\end{aligned} \tag{18}$$

The scattered electric far-field is then readily obtained as

$$\begin{aligned}4\pi r E_\theta^{far}\left(t+c^{-1}r\right) &= -c^{-1}\partial_t\left[L_\phi(\mathbf{r},t)+\eta N_\theta(\mathbf{r},t)\right] \\ 4\pi r E_\phi^{far}\left(t+c^{-1}r\right) &= -c^{-1}\partial_t\left[L_\theta(\mathbf{r},t)-\eta N_\phi(\mathbf{r},t)\right]\end{aligned} \tag{19}$$

Once the scattered field in the far region is known, the radar cross section(RCS) can be gotten from

$$\sigma = \lim_{r\to\infty} 4\pi r^2 \frac{\left|\mathcal{F}\left\{\mathbf{E}^{far}(\mathbf{r},t)\right\}\right|^2}{\left|\mathcal{F}\left\{\mathbf{E}^{inc}(\mathbf{r},t)\right\}\right|^2} \tag{20}$$

III. NUMERICAL RESULTS

One active frequency selective surface with PIN diodes is demonstrated here to show the accuracy of the proposed method. This example is a quadrate metal patches printed on a sheet of 0.04m with dielectric constant of 3.0. The typical values used for forward bias are R = 5Ω and L = 0.4 nH, while for reverse bias a series capacitance of 0.27 pF has been added to the circuit model.

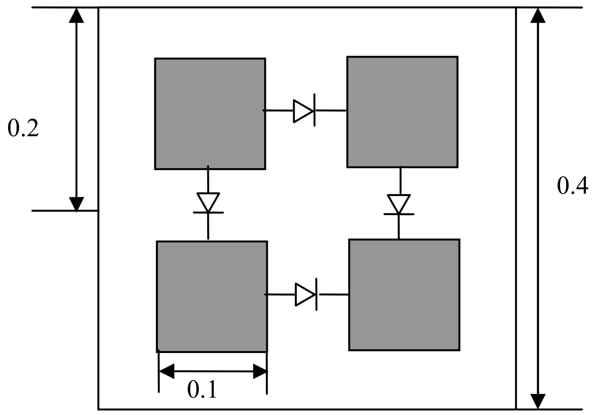

Fig.3. Structure of the active FSS with PIN diodes

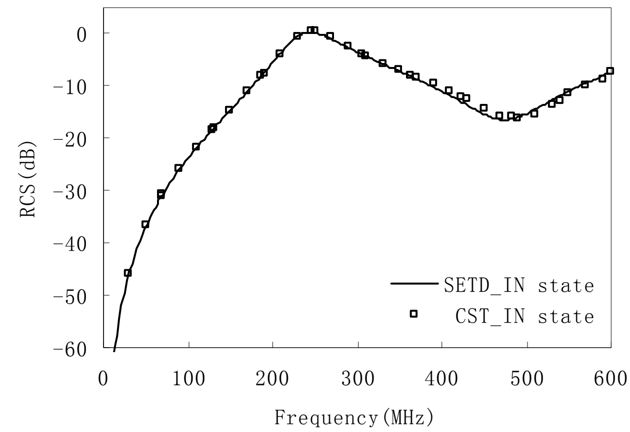

(a)

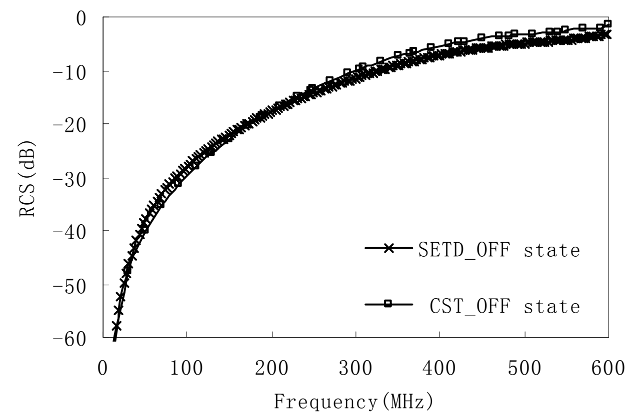

(b)

Fig.4. (a) Backscattered RCS of the active FSS when the PIN diodes are in ON state (b) Backscattered RCS of the active FSS when the PIN diodes are in OFF state

From the result, we can clearly see that the results got from the spectral-element time domain method meet well with that of the commercial software.

IV. CONCLUSION

The spectral-element time domain method has been employed to compute the scattering characteristic of the active FSS structures. Numerical results show that this method can analyze the PIN diodes-loaded FSS accurately.

ACKNOWLEDGMENT

We would like to thank the support of Major State Basic Research Development Program of China (973 Program: 2009CB320201), Natural Science Foundation of 61171041, Jiangsu Natural Science Foundation of BK2012034.

REFERENCES

[1] B.A.Munk.,Frequency Selective Surfaces,Theory and Design[M]. New York:Wiley,2000.

[2] C. Mias, "Waveguide and free-space demonstration of tunable frequency selective surface," Electronics Letters ,vol. 39, no. 11, pp. 850-852, May 2003.

[3] J.Jin, The Finite Element Method in Electromagnetics. New York:Wiley,1993.

[4] Joon-Ho Lee, Tian Xiao, and Qing Huo Liu, "A 3-D Spectral-Element Method Using Mixed-Order Curl Conforming Vector Basis Functions for Electromagnetic Fields," IEEE Transactions on Microwave Theory and Techniques.,vol.54,no.1,pp.437-444,Jan. 2006.

[5] Joon-Ho Lee and Qing Huo Liu, "A 3-D Spectral-Element Time-Domain Method for Electromagnetic Simulation," IEEE Transactions on Microwave Theory and Techniques.,vol.55,no.5,pp.983-991,May 2007.

[6] Dan Jiao, J.Jin,Eric, Michielssen, and Douglas J.Riley, "Time-domain finite-element simulation of three-dimensional scattering and radiation problems using perfectly matched layers," IEEE Trans. Antennas Propagat., vol. 51, no. 2 ,pp.296–305, Feb. 2003.